Original Research

Nicotinamide mononucleotide ameliorates acute lung injury by inducing mitonuclear protein imbalance and activating the UPR^{mt}

Shi-Han Du[1], Jia Shi[1], Tian-Yu Yu[2], Xin-Xin Hu[1], Si-Meng He[3], Ying-Ya Cao[1], Zi-Lei Xie[1], Sha-Sha Liu[1], Yu-Ting Li[1], Na Li[1] and Jian-Bo Yu[1]

[1]Department of Anesthesiology and Critical Care Medicine, Tianjin Nankai Hospital, Tianjin Medical University, Tianjin 300100, China; [2]Tianjin Medical University, Tianjin 300070, China; [3]Department of Anesthesiology and Critical Care Medicine, Tianjin Nankai Hospital, NanKai University, Tianjin 300071, China
Corresponding author: Jian-Bo Yu. Email: 30717008@nankai.edu.cn

Impact Statement

Endotoxemia resulted in excessive oxidative stress and inflammatory responses of lung tissues, and reliable prevention measure is still lacking. Nicotinamide mononucleotide (NMN) has been implicated with important roles in multiple inflammatory diseases. However, the exact effects of NMN on lipopolysaccharide (LPS)-induced lung injury and the involved mechanisms remain unclear. This study demonstrates that NMN pretreatment can ameliorate lung injury by inducing mitonuclear protein imbalance and activating the mitochondrial unfolded protein response (UPR^{mt}), which is probably regulated by deacetylase SIRT1. We therefore found a new mechanism of the protective effect of NMN and may contribute to potential use of NMN in ameliorating sepsis-associated lung injury.

Abstract

Mitochondria need to interact with the nucleus under homeostasis and stress to maintain cellular demands and nuclear transcriptional programs. Disrupted mitonuclear interaction is involved in many disease processes. However, the role of mitonuclear signaling regulators in endotoxin-induced acute lung injury (ALI) remains unknown. Nicotinamide adenine dinucleotide (NAD^+) is closely related to mitonuclear interaction with its central role in mitochondrial metabolism. In the current study, C57BL/6J mice were administrated with lipopolysaccharide 15 mg/kg to induce endotoxin-induced ALI and investigated whether the NAD^+ precursor nicotinamide mononucleotide (NMN) could preserve mitonuclear interaction and alleviate ALI. After pretreatment with NMN for 7 days, NAD^+ levels in the mitochondrial, nucleus, and total intracellular were significantly increased in endotoxemia mice. Moreover, supplementation of NMN alleviated lung pathologic injury, reduced ROS levels, increased MnSOD activities, mitigated mitochondrial dysfunction, ameliorated the defects in the nucleus morphology, and these cytoprotective effects were accompanied by preserving mitonuclear interaction (including mitonuclear protein imbalance and the mitochondrial unfolded protein response, UPR^{mt}). Furthermore, NAD^+-mediated mitonuclear protein imbalance and UPR^{mt} are probably regulated by deacetylase Sirtuin1 (SIRT1). Taken together, our results indicated that NMN pretreatment ameliorated ALI by inducing mitonuclear protein imbalance and activating the UPR^{mt} in an SIRT1-dependent manner.

Keywords: Nicotinamide mononucleotide, lipopolysaccharide, acute lung injury, mitochondrial unfolded protein response, mitochondria

Experimental Biology and Medicine **2022; 247: 1264–1276. DOI: 10.1177/15353702221094235**

Introduction

Multiple-organ failure caused by sepsis remains the leading cause of morbidity and mortality in intensive care units (ICUs).[1,2] The lung is the most susceptible organ to endotoxemia with unacceptably high mortality (34.9–46.1%).[3] Despite many in-depth studies on acute respiratory distress syndrome (ARDS) have been conducted, the specific pathogenesis of endotoxin-induced acute lung injury (ALI) remains unclear, and there are no effective pharmacological treatments.

Mitochondria are the only organelle that maintains its genome and regulates cellular energy metabolism, and mitochondrial dysfunction has shown to be tightly linked to endotoxemia lung injury.[4,5] Mitochondria have a complex communication system to alleviate their dysfunction. A variety of mitochondrial stress signals are transmitted retrogradely from mitochondria to the nucleus and initiate corresponding transcriptional adaptation responses, which allows mitochondria to keep pace with cellular demands and nuclear transcriptional programs.[6–8] For instance, the cytoprotective UPR^{mt} is activated by interference between

the mitochondrial electron transport chain subunits encoded by nuclear DNA (nDNA) and mitochondrial DNA (mtDNA), which represent mitonuclear protein imbalance.[9] Thus, inducing mitonuclear protein imbalance and activating the UPR^{mt} plays a vital part in preserving mitochondrial function in response to various cellular stressors.[10,11]

As a central cofactor, nicotinamide adenine dinucleotide (NAD^+) could modulate metabolic homeostasis and be a rate-limiting substrate for sirtuin deacetylases.[12] Multiple lines of evidence indicate that NAD^+ levels perform a crucial role in nuclear–mitochondrial interaction in aging.[6] In addition, the NAD^+ precursor NMN has been proven to enhance NAD^+ biosynthesis and ameliorate multiple pathologies in mouse disease models. Recent studies revealed that short-term administration of NMN could effectively alleviate the age-related physiological decline in mice because of mitochondrial oxidative metabolism and mitonuclear protein imbalance in skeletal muscle.[13] Furthermore, Gariani et al.[14] found that exogenous supplementation of NAD^+ activates the UPR^{mt} in the progression of non-alcoholic fatty liver disease, which is dependent upon the protein deacetylase SIRT1. Similarly, NMN could also protect mice from sepsis-induced lung and heart injury by inhibiting high mobility group box-1 release and oxidative stress via the NAD^+/SIRT1 signaling.[15] However, the molecular mechanism by which the NAD^+-related metabolisms ameliorate LPS-induced ALI has not been completely elucidated and the coordination between SIRT1 and NAD^+-mediated mitochondrial-nuclear interaction remains elusive in septic mice. Our previous researches have certified that mitochondrial morphology, dynamics, and function are impaired in endotoxin-induced ALI,[5,16,17] which may influence the interaction between mitochondria and the nucleus.

In this study, an endotoxemia mouse model was established via tail vein injection of LPS to simulate endotoxin-related lung injury. Our data indicated that NMN pretreatment can alleviate ALI by inducing mitonuclear protein imbalance and activating UPR^{mt}, which is probably regulated by deacetylase SIRT1. Rational targeting of these events may have high translational potential in endotoxin-induced ALI in which mitonuclear protein balance are implicated.

Materials and methods

Animals

A total of 98 male C57BL/6J mice (20–25 g), 6- to 8-week old were obtained from the Laboratory Animal Center of Tianjin Nankai Hospital, China. The mice were kept in cages at the indoor temperature of 23–25°C, relative humidity of 50–60%, 12-h light/dark cycle, and provided free access to standard mouse food and water. The animals were administered with pre-approval of the Animal Ethical and Welfare Committee of Tianjin Nankai Hospital (Ethic Number: NKYY-DWLL-2019-012).

Experimental design

To probe the effect of NMN on NAD^+ content in lung tissues, 25 mice were classified into five groups ($n=5$ per group): control group (group C), LPS group (group LPS), 100, 300, and 500 mg/kg/day NMN pretreatment plus LPS group. NMN was intraperitoneally given at 18:00 daily for 7 days. LPS (E.coli-L2630, Sigma, USA) 15 mg/kg were used to induce endotoxemia in mice via the caudal vein 1 h after the final administration of NMN. The mice in group C received the same volume of 0.9% sterile saline. NMN (N3501, Sigma, USA) was provided by Sigma company, and diluted in PBS and stored at –20°C until utilize. To explore the effect of NMN on endotoxemia-induced lung injury, 49 mice were randomly divided into three groups: control group (group C, $n=15$), LPS group (group LPS, $n=18$), 500 mg/kg/day NMN pretreatment plus LPS group (group LPS + NMN, $n=16$). Moreover, to further clarify the role of SIRT1 in the protective effect of NMN, 24 mice were classified into three groups ($n=8$ per group): LPS group (group LPS), NMN pretreatment plus LPS group (group LPS + NMN), and endotoxemia mice with SIRT1 inhibitor EX-527(group LPS + NMN + EX-527). In LPS + NMN + EX-527 group, mice were injected intraperitoneally with EX-527 (10 mg/kg, dissolved in dimethylsulfoxide [DMSO]) at 30 min before the last administration of NMN. And the rest of the procedures were the same as those performed in the LPS + NMN group. The dose of EX-527 was chosen based on previous studies and our preliminary experiment.[18,19]

All the mice were sacrificed by cervical dislocation under deep anesthesia at 12 h after LPS injection. A portion of lung tissues was placed in 4% paraformaldehyde for pathological analyses. The remaining lung tissues were collected and stored at –70 °C for further observation or measurement. The survival rates in each group were examined before they were sacrificed.

NAD^+ measurement

NAD^+ content was quantified with a commercial available kit (ab65348, Abcam, USA) according to the manufacturer's instructions. The lungs of mice were removed rapidly and weighed. The isolated mitochondrial and nuclear fraction from lung tissues was conducted as before.[20,21] The final mitochondrial and nuclear pellet was gently re-suspended, homogenized, and transferred into Eppendorf (EP) tube with extraction buffer. NAD^+ total and NADH content was quantified by iMark™ Microplate Absorbance Reader (BIO-RAD) at 450 nm. The NAD^+ content was equal to the NAD^+ total content minus the NADH content.

Histological examination

Twelve hours after LPS or normal saline injection, mice were sacrificed and quickly separated the right upper and right middle lung lobes. The surface bloodstains were washed away at 4°C with phosphate-buffered saline (PBS) and immersed in 10% paraformaldehyde solution. Subsequently, the tissues were routine dehydration, paraffin-embedded, and made into 4 μm slices. Lung sections were stained with hematoxylin and eosin (H&E), then were observed, and scored by blinded investigators. Fifteen visual fields of each section were selected from the sections under a light microscope (×200 magnification). The severity extent of lung injury was assessed according to the pathologic scoring

Table 1. Real-time RT-PCR primers.

Gene	Forward	Reverse
Hsp60	5'-GCCTTAATGCTTCAAGGTGTAGA-3'	5'-CCCCATCTTTTGTTACTTTGGGA -3'
GAPDH	5'-GTCGTGGAGTCTACTGGTGTC -3'	5'-GAGCCCTTCCACAATGCCAAA -3'
mtDNA	5'-CCCAGCTACTACCATCATTCAAGT-3'	5'-GATGGTTTGGGAGATTGGTTGATG-3'
Actin	5'-GTACCACCATGTACCCAGGC-3'	5'-GCAGCTCAGTAACAGTCCGC-3'

criteria: inflammation infiltration or aggregation, intra-alveolar congestion, hemorrhage, and alveolar wall thickening. The grading scale is: 0, minimal; 1, mild; 2, moderate; 3, severe; and 4, maximal.[22]

Measurement of reactive oxygen species

The left lower lung tissue was digested with trypsin and then filtered through a 200-mesh sieve to generate a cell suspension. The levels of reactive oxygen species (ROS) were evaluated by 2'-7'dichlorofluorescin diacetate (DCFH-DA) probe for 30 min at 25°C and washed three times to remove redundant probes. The fluorescence signal was excited at 485 nm and the fluorescent signals were detected at 520 nm by a microplate reader. The relative ROS levels were presented as a percentage compared to the control.

Manganese superoxide dismutase activity

The left upper lung tissue was used to measure the enzymatic activity of manganese superoxide dismutase (MnSOD) in the mitochondria by superoxide dismutase (SOD) typed assay kit (A001-2-2, Nanjing Jiancheng Bioengineering Institute, Nanjing, China). The results are represented in units per milligram of protein (U/mg protein).

Detection of mitochondrial membrane potential ($\Delta\Psi$m)

The right lung tissues were minced with scissors and digested with collagenase for 30 min at 37 °C. Detached cells were re-suspended in 1 ml Hanks' balanced salt solution (HBSS) and centrifuged at 400 g for 5 min. Then, the cells were washed and incubated with JC-1 (10 μg/mL, BD Biosciences) at 37°C for 30 min. After that, cells were washed and re-suspended in 500 μL 1× assay buffer. The levels of $\Delta\Psi$m were analyzed by flow cytometry (BD Biosciences) using appropriate gate settings and the changes of $\Delta\Psi$m calculated as the ratio of bright red/green fluorescence.

Terminal deoxynucleotidyl transferase (TdT) dUTP nick-end Labeling assay

The left upper lung tissue was utilized to detect apoptosis according to the instructions of the terminal deoxynucleotidyl transferase (TdT) dUTP nick-end labeling (TUNEL) kit (Roche Applied Science). Photos were captured with a fluorescence microscope (Olympus IX71). Ten fields were randomly selected to count TUNEL-positive cells on each slide and the average value of them was calculated (original magnification ×400).

Cytochrome c oxidase activity

The left lower lung tissue was used to determine the enzyme activity by cytochrome c oxidase (COX) assay kit (CYTOCOX1, Sigma-Aldrich, USA) following the manufacturer's instructions. Samples were read at 550 nm and the cytochrome oxidase activity values were expressed as μmol of oxidized cytochrome c/min/mg of protein. The bicinchoninic acid assay (BCA) method was used to measure protein concentrations.

Transmission electron microscopy

Ultrastructural changes in pulmonary mitochondria were assessed by transmission electron microscopy (TEM). The right lung tissue sections were fixed in 2.5% glutaraldehyde at 4°C overnight and washed three times with phosphate buffer. The specimens were post-fixed with 1% osmium tetroxide for 2 h. After graded dehydration in a series of ethanol, the samples were embedded in acetone. The embedded tissues were sectioned at a thickness of 70 nm and stained with 4% uranyl acetate and lead citrate. Last, the specimens were observed by TEM (Tecnai G2, FEI).

Mitochondrial DNA content

The DNeasy Blood and Tissue Kit were used to isolate total DNA from left upper lung tissues (#DN10, Aidlab Biotechnologies). Real-time PCR (RT-PCR) was performed with SYBR-green PCR master mix. The relative expression of the mtDNA content was based on the $2^{-\Delta\Delta CT}$ method. The primer sequences of mtDNA and nuclear-encoded actin are listed in Table 1.

Quantitative real-time reverse transcription polymerase chain reaction (qRT-PCR)

The RNA Extraction kit (Invitrogen, Carlsbad, CA) was used to extract total RNA from right lower lung tissues according to the manufacturer's protocol. The extracted RNA was reverse transcribed into complementary DNA (cDNA) with a High-Capacity cDNA RT kit (EP0442, Thermos Fisher, USA). The relative mRNA levels for HSP60 were performed with SYBR-green PCR master mix (Q511-02, Vazyme Biotech, CN). Glyceraldehyde 3-phosphate dehydrogenase (GAPDH) was employed as the internal control for HSP60. The relative expression was based on the $2^{-\Delta\Delta CT}$ method. The primer sequences are shown in Table 1.

Western blotting assay

Total protein was extracted from left lower lung tissues with radioimmunoprecipitation assay (RIPA) lysis buffer and

quantified using a protein quantitation Kit (Bio-Rad, CA, USA). The protein extracts (40 μg) were subjected to 10% SDS-PAGE, followed by transferring to a polyvinylidene difluoride (PVDF) membrane. Each PVDF membrane was incubated with 5% defatted dry milk for 2 h and then probed with primary antibodies overnight at 4°C. Included anti-SIRT1 (1:1000, bs-0921R, Bioss, CN), anti-MTCO1 (1:2000, ab14705, Abcam, UK), anti-succinate dehydrogenase A (SDHA) (1:1000, ab14715, Abcam, UK), and anti-GAPDH (1:2500, TA-08, ZSGB-BIO, CN). The membranes were washed with Tris-buffered saline solution with Tween (TBST) three times before the incubation with horseradish peroxidase-labeled goat anti-rabbit immunoglobulin G (IgG) secondary antibodies (1:2500, ZB-2301, ZSGB-BIO, CN) and goat anti-mouse IgG secondary antibodies (1:2500, ZB-2305, ZSGB-BIO, CN) at 25°C for 1 h. Finally, the protein bands were visualized using the enhanced chemiluminescence-detection system (Bio-Rad, CA, USA) and analyzed with Image J. Mitonuclear protein imbalance (mtDNA:nDNA ratio) was determined by the ratio of mitochondrial-encoded MTCO1 (complex IV) to nuclear-encoded SDHA (complex II) as described previously.[13,23]

Statistical analysis

The data were presented as the mean (standard deviation, *SD*). The results were analyzed by Statistical Program for Social Sciences 26.0 software (SPSS, Inc.) and GraphPad Prism 8.3 software (GraphPad Software, Inc.). One-way analysis of variance (ANOVA) combined with Bonferroni correction was used for analyzing differences between multiple groups. Kaplan–Meier survival analysis was used to analyze the survival rate by the log-rank test. A p-value < 0.05 was considered as significant.

Results

Supplementation of NMN increased NAD^+ levels in endotoxemia ALI mice

As a key precursor of NAD^+ (Figure 1(a)), NMN has been demonstrated to be beneficial in several diseases by restoring NAD^+ levels.[24,25] According to the effective doses of NMN in previous studies ranging from 62.5 to 500 mg/kg/day by intraperitoneal injections.[26] Thus, 100, 300, and 500 mg/kg/day were, respectively, chosen as the low, medium, and high dosages in our research to assess the optimal dose of NMN up-regulated NAD^+ level in lung tissues of endotoxemia mice. Mice were daily supplemented with different doses of NMN (100, 300, 500 mg/kg/day) intraperitoneally for 7 days and then LPS were intravenously injected 1 h after NMN pretreatment (Figure 1(b)). As shown in Figure 1(c), a marked increase in the total NAD^+ levels was detected in lung tissues from endotoxemia mice relative to controls. Moreover, we observed a further increase of NAD^+ in mice with NMN pretreatment (Figure 1(c)). Next, we detected the NAD^+/NADH ratio to investigate whether the redox state was influenced, which is universal application in previous studies.[27] The ratio of NAD^+/NADH was increased in LPS-challenged mice and was furtherly elevated after NMN pretreatment (Figure 1(c)). Furthermore, NAD^+ levels were enhanced more than two-fold and the NAD^+/NADH ratio was also dramatically increased in isolated mitochondria from NMN-pretreated endotoxemia mice (Figure 1(d)). Similarly, NMN enhanced NAD^+ biosynthesis in the isolated nucleus of mice and elevated NAD^+/NADH ratio in total (Figure 1(e)). Hence, the selected dose of NMN in subsequent experiments was 500 mg/kg/day, similar to previous studies.[28] Specifically, the ratio of mitochondrial NAD^+ contents/ nuclear NAD^+ contents increased in mice after the pretreatment with NMN compared with the other two groups, which indicated that the elevation of NAD^+ contents was more pronounced in mitochondria than in the nucleus (Figure 1(f)). Although there was an ascending trend in the LPS group, the difference was not statistically significant.

NMN prevented oxidative damage and alleviated lung injury in endotoxemia mice

To determine the effect of NMN on oxidative damage in mice stimulated with LPS, we first detected the survival rate in endotoxemia mice. The Kaplan–Meier survival analysis exhibited NMN pretreatment prolonged survival compared with the group treated with LPS alone (Figure 2(a)). Histological analysis manifested severe leukocyte infiltration, alveolar wall thickening, intra-alveolar hemorrhage, and congestion in the lung from mice, which were greatly alleviated in the NMN-pretreated mice (Figure 2(b)). Quantitatively, the lung injury scores were also dramatically reduced by NMN in endotoxemia mice (Figure 2(b)). Next, we examined the production of ROS and the activity of MnSOD in lung tissues of mice. Consistent with previous studies, LPS resulted in increased ROS levels but decreased MnSOD activities in the lung tissue of mice compared with the control group.[5] In contrast, mice supplemented with NMN showed decreased ROS production and increased MnSOD activity (Figure 2(c) to (d)). Furthermore, cell apoptosis mechanism in pulmonary tissues is involved in the progression of lung injury during sepsis.[29] Similarly, we found that LPS increased TUNEL-positive cells in mice, whereas the increase of apoptotic cells was markedly attenuated by NMN pretreatment (Figure 2(e) and (f)).

NMN supplementation restored mitochondrial function in mice challenged by LPS

Mitochondrial morphological and functional impairment is involved in LPS-induced lung injury.[17,30] To investigate whether NMN supplementation could improve mitochondria functions in endotoxemia mice. Mitochondrial membrane potential, cytochrome oxidase activity, and mitochondrial DNA contents that were identified as symbolic indicators of mitochondrial function were analyzed in lung tissues of mice.[31] As shown in Figure 3(a) and (b), JC-1 fluorescence was detected in red and green channels in control, while $\Delta\Psi m$ in mice lung tissues exhibited a significantly lower level as indicated by the increased green fluorescence and decreased red fluorescence. However, pretreatment with NMN markedly ameliorated LPS-induced mitochondrial membrane potential decline in mice lung tissues (Figure 3(a) and (b)). Because mitochondrial proliferation is an early

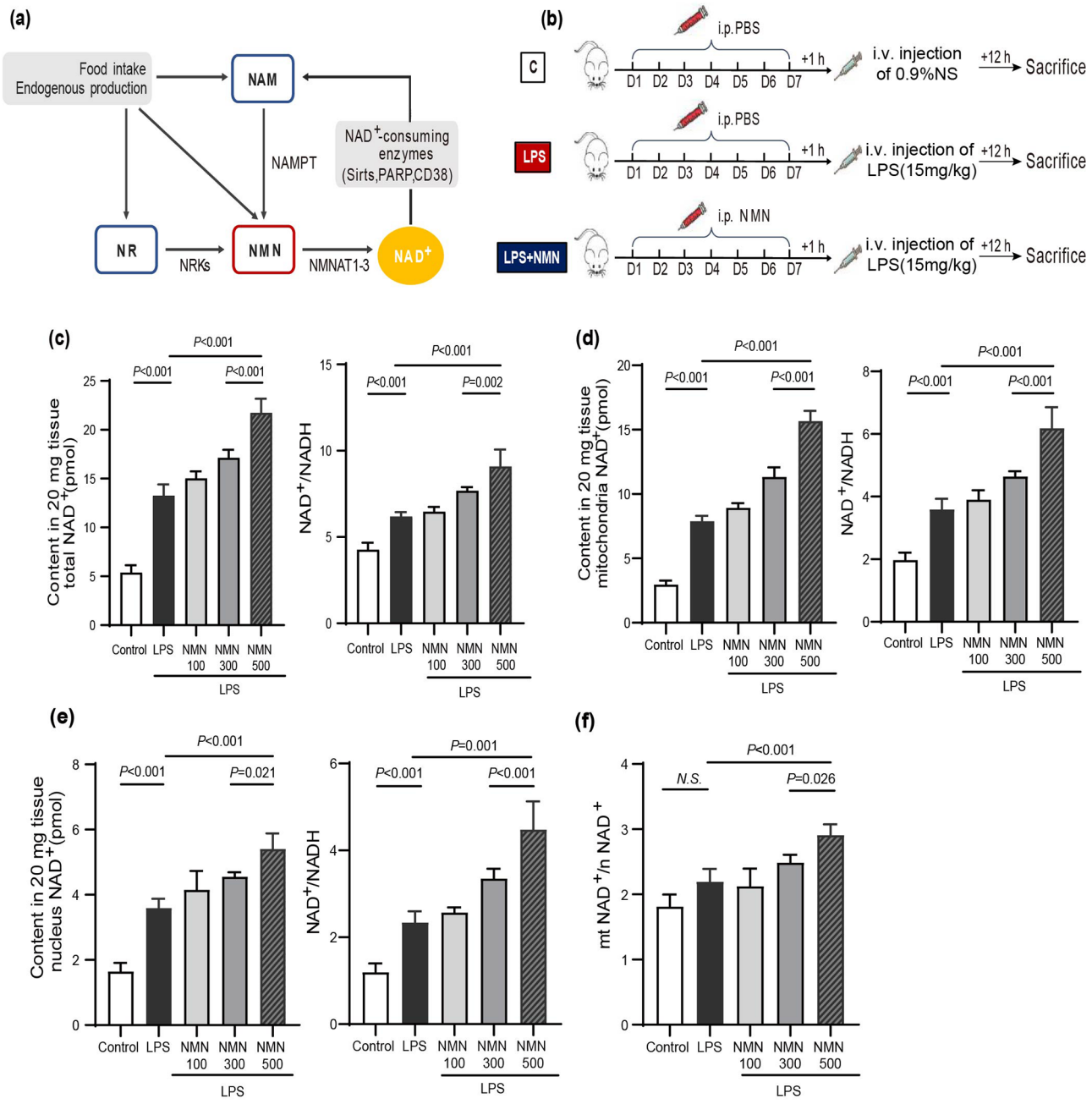

Figure 1. Administration of NMN increased NAD⁺ levels in mice challenged by LPS. (a) NAD⁺-biosynthesis salvage pathways and NAD⁺ catabolism. (b) The animal experimental flowchart. C57BL/6 mice (20–25 g) were subjected to different doses of NMN (100, 300, and 500 mg/kg/day) or PBS intraperitoneally at 18:00 daily for 7 days. LPS (15 mg/kg) or 0.9% normal saline were injected via caudal vein, respectively, after 1 h. Then, mice were sacrificed 12 h after LPS injection and lung tissues were collected. (c) Pulmonary total NAD⁺ contents and ratios of NAD⁺/NADH in mice. (d) Mitochondrial NAD⁺ contents and ratios of NAD⁺/NADH in mice in each group. (e) Nuclear NAD⁺ contents and ratios of NAD⁺/NADH in mice in each group. (f) The ratios of mitochondrial NAD⁺ contents/ nuclear NAD⁺ contents in mice in each group. Statistical difference was calculated by one-way ANOVA ($n = 5$/group). (A color version of this figure is available in the online journal.)

cellular stress response, we next quantified mitochondrial DNA content in lung tissues. A slight but statistically not significant increase in mtDNA content was observed in endotoxemia mice, whereas, a significant increase in mice pretreatment with NMN (Figure 3(c)). COX activity, the terminal oxidase of the mitochondrial electron transport chain, which was measured as an index of complex IV function in multiple studies.[29,30] Furthermore, we measured the enzymatic activity of COX in each group. As shown in Figure 3(d), the enzymatic activities of COX were significantly decreased in mice challenged by LPS compared to controls, and the pretreatment of NMN was able to profoundly enhance the enzymatic activity (Figure 3(d)). TEMs were used to investigate the effect of NMN on mitochondria and nucleus morphology. In control mice, mitochondria manifested as a typical filamentous shape with integrated double membranes and tight cristae. Whereas, the mitochondrial morphology of lung tissues in endotoxemia mice exhibited significant changes, including swollen and vacuolated mitochondria with altered cristae density, while NMN

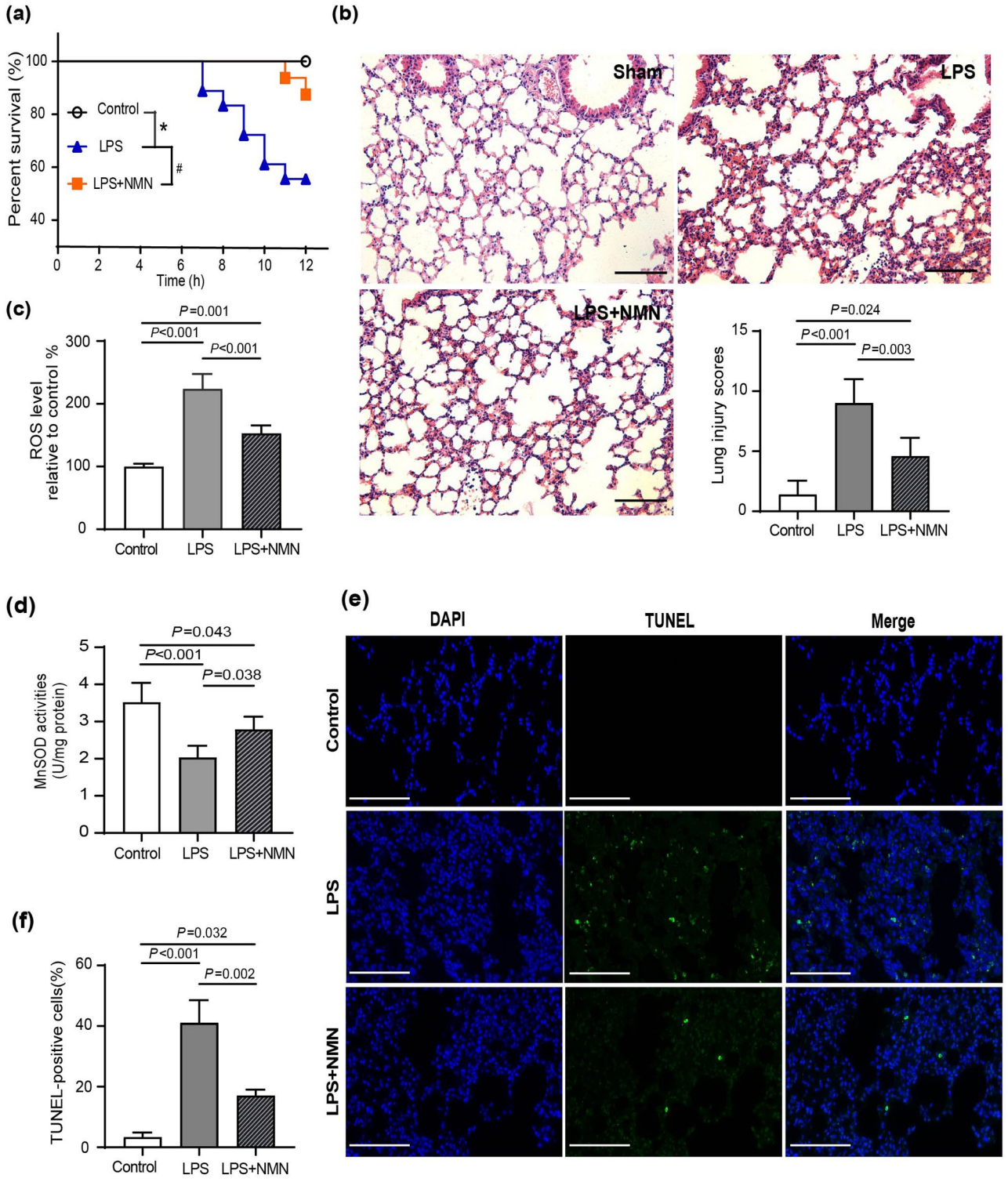

Figure 2. NMN prevented oxidative damage and alleviated lung injury in endotoxemia mice. (a) The Kaplan–Meier survival curve for NMN pretreated mice and PBS pretreated mice after LPS administration. $n = 15$ for the control group, $n = 18$ for the LPS group, $n = 16$ for the LPS + NMN group, $^{\#}p < 0.05$, $^{*}p < 0.01$. (b) HE staining and corresponding lung histology scores. Scale bar, 100 μm. (c) ROS levels. (d) MnSOD activity. Statistical difference was calculated by one-way ANOVA ($n = 5$/group). (e) Representative TUNEL staining of formalin-fixed lung sections. Scale bar, 100 μm and (f) counted percentages of TUNEL-positive cells ($n = 3$/group, Power calculation for statistic differences between groups = 1). (A color version of this figure is available in the online journal.)

pretreatment attenuated the mitochondrial damage in endotoxemia mice (Figure 3(e)). Moreover, in mice challenged by LPS, we not only found unusual nucleus sizes and shapes but also found irregular nuclear membrane and pyknotic nuclei. As expected, NMN pretreatment maintains the normal morphology of the nucleus (Figure 3(e)).

NMN mitigated lung injury accompanied by a mitonuclear protein imbalance and activation of the UPR^{mt} in endotoxemia mice

Previous studies have shown that part of the beneficial effects of NAD$^+$ may due to the existence of mitonuclear

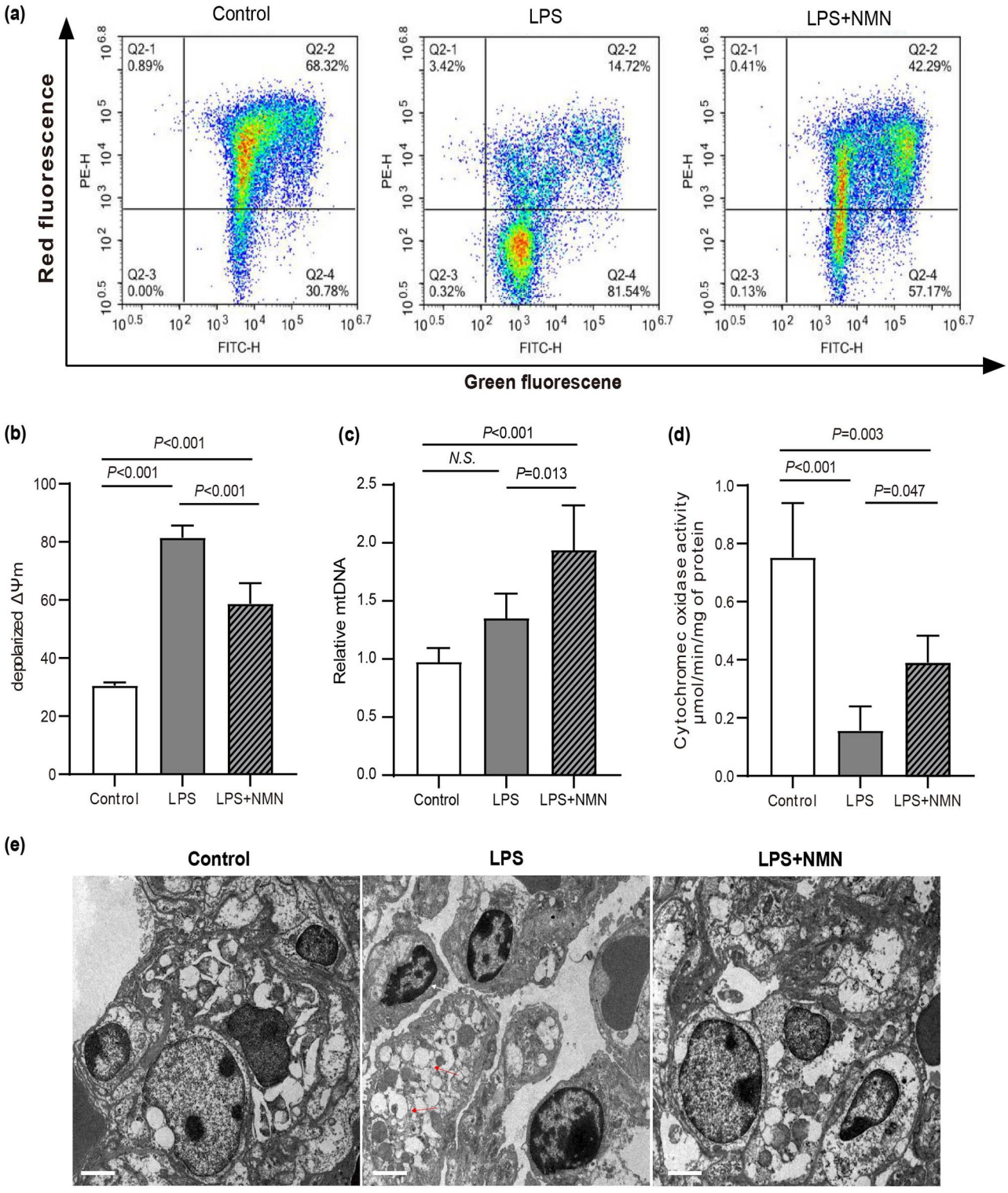

Figure 3. Effects of NMN on mitochondrial function. (a) Mitochondrial membrane potential (ΔΨm) analyzed by flow cytometry. Q2-2, red fluorescence+/green fluorescence+, polarized ΔΨm; Q2-4, red fluorescence–/green fluorescence+, depolarized ΔΨm. (b) Quantitative histogram of ΔΨm. (c) Relative mtDNA content using real-time PCR. (d) Cytochrome c oxidase activity in mice. Statistical difference was calculated by one-way ANOVA ($n=5$/group). (e) The morphological alterations of mitochondria and the nucleus were observed by transmission electron microscopy. Scale bars, 2 μm. Red arrows denoted abnormal mitochondria, which were manifested as isolated, swollen, and vacuolization mitochondria without clear cristae. White arrows denoted unusual nucleus size and shape, pyknotic nuclei, and irregular nuclear membrane. All the results were obtained from three independent experiments. (A color version of this figure is available in the online journal.)

protein imbalance (mtDNA-encoded mitochondrial proteins and nDNA-encoded mitochondrial proteins).[6,13] Thus, we calculated the ratios of the cytochrome c oxidase subunit I (MTCO1), oxidative phosphorylation (OXPHOS) subunit encoded by the mtDNA, to SDHA, an OXPHOS subunit encoded by the nDNA.[13] Indeed, NMN administration increased the ratios of MTCO1/SDHA, which suggests the development of a mitonuclear protein imbalance

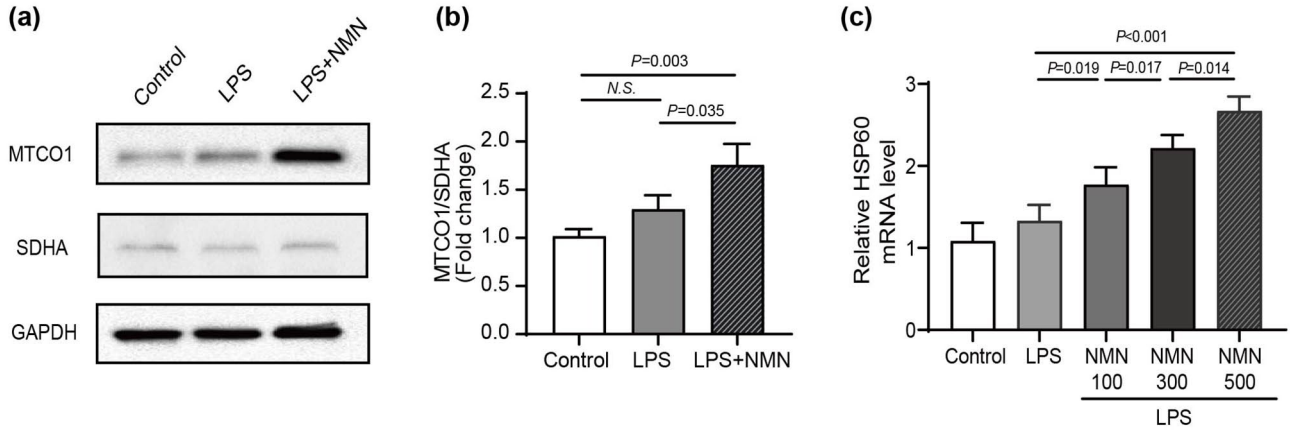

Figure 4. NMN mitigated LPS-induced oxidative injury by inducing mitonuclear protein imbalance and activating the UPR^{mt} in mice. (a) The protein levels of mtDNA-encoded and nuclear DNA-encoded mitochondrial proteins (MTCO1, SDHA) from the lung tissues of mice. (b) The protein ratios of MTCO1 to SDHA ($n=3$/group, Power calculation for statistic differences between groups = 0.987). (c) qRT-PCR assay was applied to detect the mRNA expression levels of HSP60 ($n=5$/group). Statistical difference was calculated by one-way ANOVA. HSP60, heat shock protein 6; MTCO1, cytochrome c oxidase subunit I; SDHA, succinate dehydrogenase A.

(Figure 4(a) and (b)). Besides, the mitonuclear protein imbalance could activate UPR^{mt}, an adaptive response to maintain mitochondrial proteostasis and ultimately repair hermetic signaling pathways.[32] The mRNA levels of HSP60 in mitochondrial chaperone systems were commonly used to evaluate the UPR^{mt} in mice. Because of the mitonuclear protein imbalance, the mRNA expression level of HSP60 up-regulated in endotoxemia mice compared to control. Furtherly, the relative expression value of HSP60 mRNA progressively increased with NMN concentrations (Figure 4(c)). Taken together, these findings suggested that NMN protects against lung injury in endotoxemia mice by inducing mitonuclear protein imbalance and activating the UPR^{mt}.

NMN alleviated LPS-induced ALI in an SIRT1-dependent manner

The NAD$^+$-dependent class III histone deacetylase SIRT1 is preferentially located in the nucleus and likely contributes to the modulation of chromatin and the DNA damage response.[33] Since previous studies have clarified the critical role of SIRT1 in LPS-induced ALI,[34] we wonder if the protective effects of NMN are linked to SIRT1 activation. Therefore, we performed immunoblotting assay to examine NAD$^+$-dependent SIRT1 expression level. As shown in Figure 5(a), NMN pretreatment up-regulated protein expression of SIRT1 in the context of LPS induced acute lung inflammation (Figure 5(a)). To further substantiate that SIRT1 action mediated the effects of NMN, SIRT1 expression in endotoxemia mice was inhibited by EX-527, a potent and specific SIRT1 inhibitor. As expected, H&E staining and the lung injury score showed that NMN could not attenuate pathological injury after SIRT1 inhibition by EX-527 (Figure 5(b)). Meanwhile, SIRT1 inhibition also counteracted the antioxidant effects from NMN in mice with ALI, which was evidenced by the decreased MnSOD activity (Figure 5(c)). Furthermore, we detected mitochondrial DNA content and mitochondrial ultrastructure in mice after SIRT1 inhibition to elucidate mitochondrial damage. The beneficial morphological changes of mitochondria following NMN treatment were considerably blocked by EX-527 addition (Figure 5(d)). And, the mtDNA copy number was decreased following EX-527 treatment compared with mice without EX-527 treatment (Figure 5(e)). Next, we also evaluated mitonuclear protein imbalance and UPR^{mt} activation in mice after SIRT1 inhibition. We found that administration of NMN displayed mitonuclear protein imbalance—the increased ratio between mtDNA- and nDNA-encoded OXPHOS proteins—activated UPR^{mt} response as judged by Hsp60 expression, while these effects were reversed when SIRT1 was inhibited (Figure 5(f) to (h)).

Discussion

Given the high morbidity and mortality of ARDS, there is an urgent requirement to identify effective treatments for sepsis-induced lung injury. In the current study, we confirmed that pretreatment with NMN, an NAD$^+$ precursor, could significantly increase NAD$^+$ contents and attenuated lung injury in mice challenged by LPS. Our data also indicated that the protective effect of NMN may be achieved by inducing mitonuclear protein imbalance and activating the UPR^{mt} in an SIRT1-dependent manner and thus improving mitochondrial function and endotoxemia-associated inflammation (Figure 6).

NAD$^+$ is a key intermediate in several metabolic pathways, such as glycolysis, tricarboxylic acid cycle, fatty acid oxidation, and oxidative phosphorylation, as well as mitochondrial biogenesis and so on.[35] NAD$^+$ is thought to be impermeable to the plasma membrane and is easily degraded by serum hydrolases, making it difficult to be replenished directly.[36] Therefore, the NAD$^+$ precursor NMN is harnessed for increased NAD$^+$ contents in rodents and humans. NMN supplementation was regarded as an effective therapy to protect against cell death, inflammatory disease and obesity.[37–39] Previous studies revealed a reduction in NAD$^+$ levels in lung tissues of endotoxemia mice.[15] However, some studies provided inconsistent conclusions of those described above. These studies have shown that the cellular NAD$^+$ contents initially decrease after LPS treatment and then gradually increase for up to 24 h.[37] Similarly, our current study also indicated that LPS led to enhanced total NAD$^+$ contents,

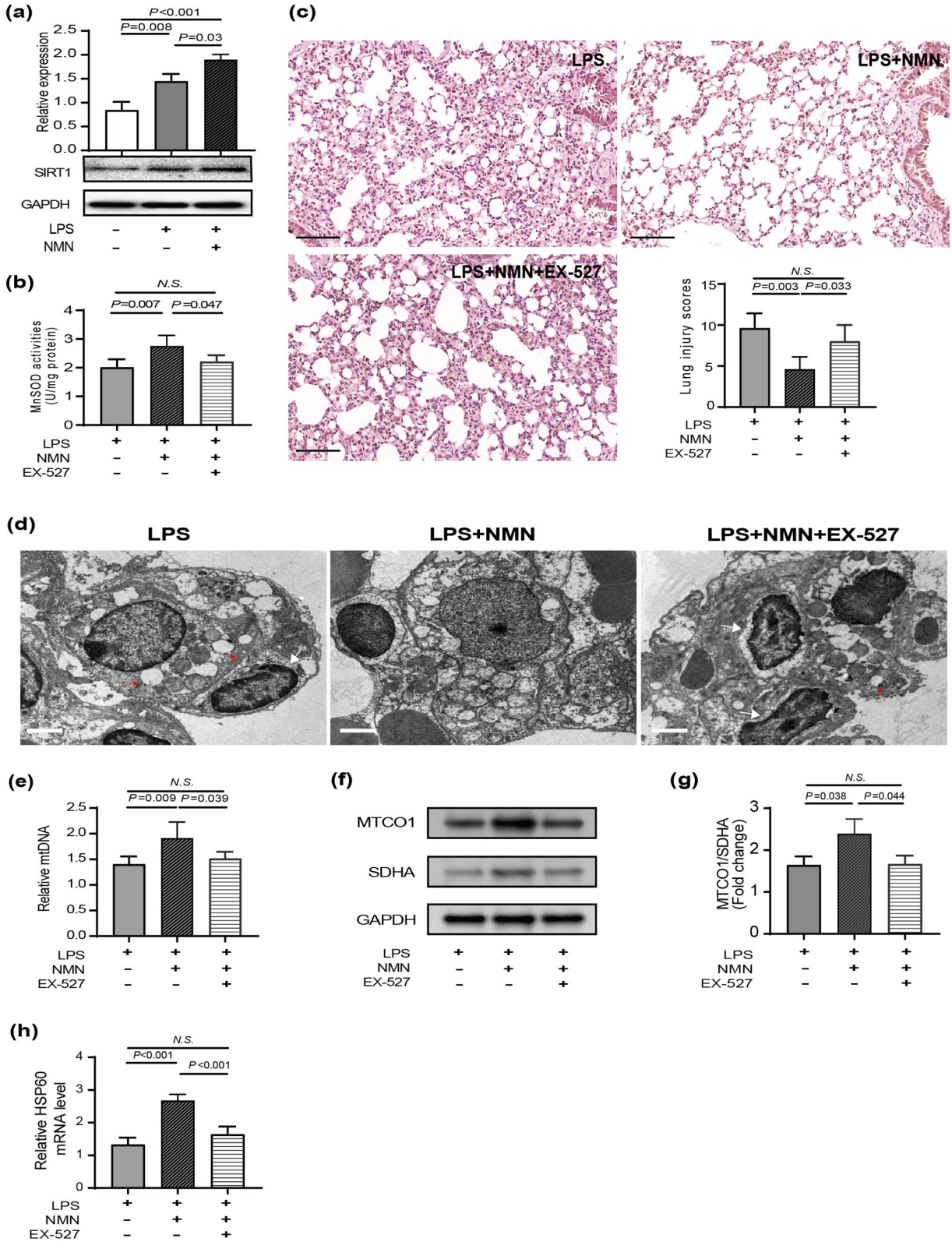

Figure 5. NMN protected LPS-induced acute lung injury in an SIRT1-dependent manner. (a) Representative immunoblots of SIRT1 in lung tissues ($n=3$/group, power calculation for statistic differences between groups = 0.999). (b) HE staining and corresponding lung histology scores. Scale bar: 100 μm. (c) MnSOD activity ($n=5$/group). (d) The morphological alterations of mitochondria and the nucleus were observed by transmission electron microscopy. Scale bars, 2 μm. Red arrows denoted abnormal mitochondria, which were manifested as isolated, swollen, and vacuolization mitochondria without clear cristae. White arrows denoted unusual nucleus size and shape, pyknotic nuclei, and irregular nuclear membrane. All the results were obtained from three independent experiments. (e) Relative mtDNA content using real-time PCR ($n=5$/group). (f) The protein levels of MTCO1 and SDHA from lung tissues of mice. (g) The protein ratios of MTCO1 to SDHA ($n=3$/group, Power calculation for statistic differences between groups = 0.830). (h) qRT-PCR assay was applied to detect the mRNA expression levels of HSP60 ($n=5$/group). Statistical difference was calculated by one-way ANOVA. (A color version of this figure is available in the online journal.)

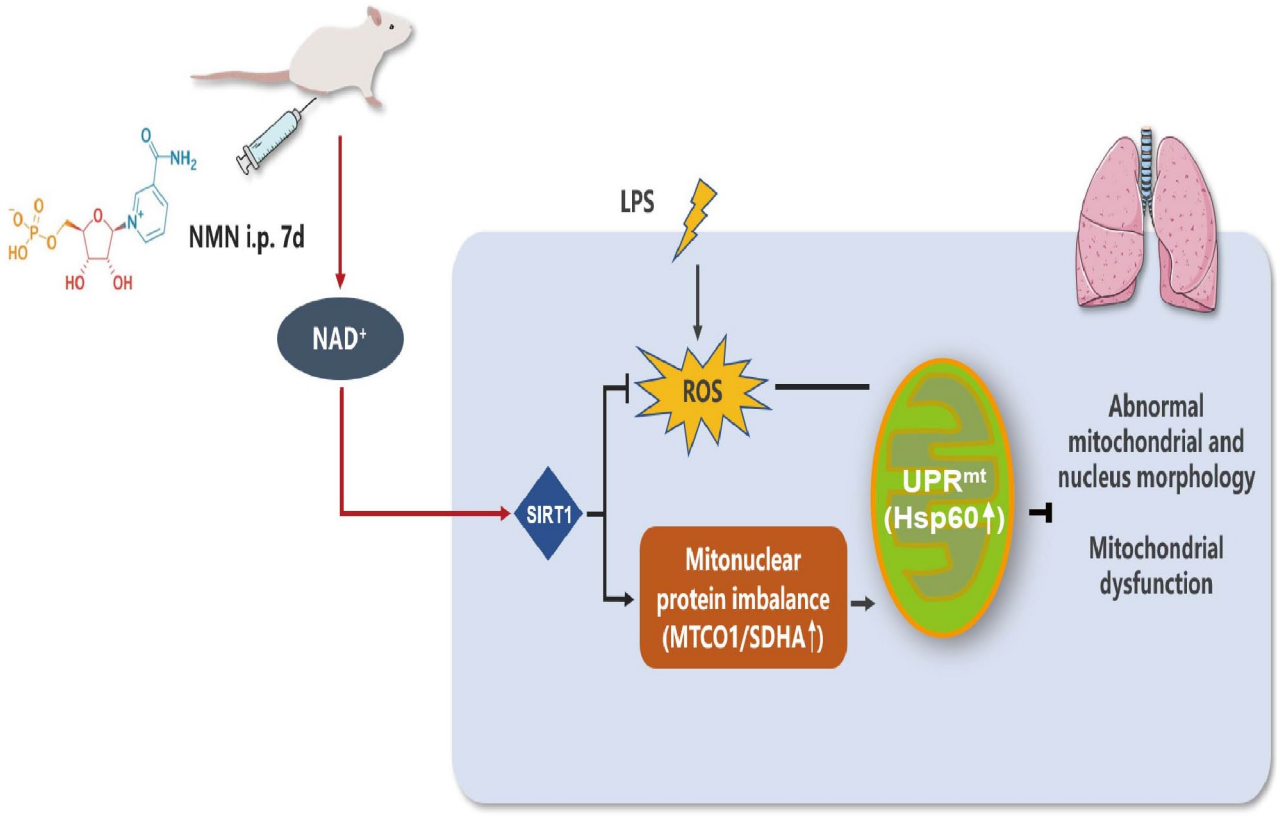

Figure 6. Protective effects of NMN on LPS-induced acute lung injury and the underlying mechanism. When LPS was administrated to C57BL/6J mice induced the production of a large amount of ROS. Meanwhile, pretreatment with NMN increased the levels of NAD^+, up-regulated SIRT1 expression, improved mitochondrial morphology and dysfunction, accompanied by inducing mitonuclear protein imbalance and activating the mitochondrial unfolded protein response in endotoxemia mice. Thus, NMN administration might be an effective strategy for preventing endotoxemia-induced lung injury. (A color version of this figure is available in the online journal.)

mitochondrial NAD^+ as well as nuclear NAD^+ contents in lung tissues of mice. The increase in NAD^+ may be attributed to differences in the duration of LPS stimulation in mice among these studies or the activation of endogenous antioxidant defenses.

To explore the influence of NAD^+ on endotoxin-induced ALI, we not only compared pathological sections and the lung injury scores among three groups, but also evaluated the effects of NMN supplementation on the degree of oxidative stress. Our results demonstrated that pretreatment with NMN significantly decreased lung injury scores, mitigated the degree of oxidative damage by reducing ROS production and increasing the activity of MnSOD, which was consistent with other studies.[5,40] Next, we analyzed mitochondrial function after NMN pretreatment in endotoxemia mice. In agreement with previous studies,[17,41] more swollen and vacuolated mitochondria and abnormally shaped nucleus were observed in endotoxemia mice. The impaired mitochondrial morphology was related to decreased $\Delta\Psi m$. Normal mitochondrial membrane potential is a prerequisite for oxidative phosphorylation and ATP production process, as well as a necessary condition for maintaining mitochondrial function.[42,43] Our data showed that compromised mitochondrial and nuclear morphology and declined $\Delta\Psi m$ were ameliorated after NMN administration. COX, also known as complex IV, is a terminal enzyme of the mitochondrial electron transport chain. COX phosphorylation and reduced mitochondrial potential were found in the sepsis rat model.[44] In line with these findings, the present data showed lower COX activity in septic mice compared to control. And COX activity increased after replenishing NAD^+ compared to the LPS group. In addition, mtDNA damage induced by endotoxin was involved in mitochondrial dysfunction and ultrastructural damages.[45] Our study reflected that mtDNA levels significantly increased after NMN supplementation in endotoxemia mice, supporting that the mitochondrial biosynthesis enhanced. Taken together, pretreatment with NMN effectively alleviated the LPS-induced lung injury through suppression of oxidative stress-mediated mitochondrial impairment.

NAD^+ participates in the homeostasis between mitochondria and nucleus as a small molecule during ALI. Moreover, NAD^+ acts as a substrate for poly (ADP-ribose) polymerases (PARPs) and class III NAD-dependent deacetylases (SIRTs), modulating their activities.[46] The concentrations of NAD^+ and NADH in mitochondria influence the distribution of NAD^+ in the nucleus.[6,47] Except for some protein-coding genes in vestigial circular mitochondrial DNA, most mitochondrial-coding genes are translocated into the nucleus, indicating that mitochondria and the nucleus interact with each other to ensure optimal cellular function.[48] Compromised mitonuclear interaction is implicated in metabolic diseases, neurodegeneration, cancer, and other aging processes, but little is known about mitonuclear signaling

regulators in endotoxin-induced lung injury. To confirm the protective effect of NMN on lung injury from the perspective of mitonuclear interaction, we investigated mitonuclear protein imbalance and UPR^{mt}. The mismatch between the nDNA- and mtDNA-encoded subunits of mitochondrial components is the characteristic of a mitonuclear protein imbalance that has been proven to activate UPR^{mt}. In addition, the unfolded protein stresses trigger UPR^{mt} in turn and aim to normalize the mitonuclear protein imbalance by assisting in protein folding and degradation.[49] In the current study, the ratio between the two proteins (MTCO1/SDHA) increased in endotoxemia mice pretreatment with NMN, suggesting that the mitonuclear protein imbalance was induced. Moreover, the abundance of HSP60, a key protein chaperone of the UPR^{mt}, presented a medium-increase in endotoxemia mice, and intraperitoneal administration of NMN induced much higher expression levels.

Previous studies have demonstrated that nicotinamide riboside could prevent non-alcoholic fatty liver disease, enhances hepatic-oxidation and mitochondrial complex content and activity. These events rely on the protein deacetylase SIRT1 and involve the mitonuclear protein imbalance as well as activation of stress signaling via the UPR^{mt}.[14] Remarkably, multiple lines of evidence support the contribution of SIRT1 in protecting against ALI in endotoxemia mice.[50,51] Thus, we examined the roles of SIRT1 in the activation of UPR^{mt} in endotoxemia mice. For the current study, we observed that NMN up-regulated the hallmark of the UPR^{mt}(HSP60) through up-regulation of SIRT1, while down-regulation of SIRT1 counteracted the role of NMN in activating UPR^{mt}. These data imply that SIRT1-UPR^{mt} exerts positive effects in promoting the restoration and recovery of mitochondrial ultrastructure and function.

The current study still has some limitations. First, we only detected the expression levels of the OXPHOS subunit encoded by mitochondria and nuclear, but were unable to observe the dynamic interaction between mitochondria and nuclear. Hence, newer technologies (e.g. Imaging mass cytometry) may make these studies more convincing in the future. Second, our research lacks the experimental group of endotoxemia mice with NMN post-conditioning, which is more approach to the real clinical treatment with drugs. Future studies should establish NMN post-conditioning group and compared the effect between NMN pre-conditioning group and post-conditioning group in a mouse endotoxin-induced ALI model. Third, we just observed the changes of nuclear morphologies without examining the indicators that reflect the nuclear function, such as transcriptional regulation in the current study. Finally, the efficacy and safety of NMN on patients with endotoxemia-associated lung injury have not yet been validated clinically. Notably, long-term intake of NMN is well-tolerated without side effects in laboratory animals.[13] Although relatively few clinical trials in septic patients have been reported, the trial from Japan had been accomplished to assess the tolerability of NMN in aging humans which aimed to develop NMN as an anti-aging nutraceutical.[51] Therefore, in patients with sepsis, clinical trials of NMN supplementation are feasible in the future, which would contribute to the potential use of NMN in ameliorating endotoxin-associated ALI.

In conclusion, the present study showed that NMN ameliorated endotoxin-induced ALI in vivo by inducing mitonuclear protein imbalance and activating the UPR^{mt}, which is probably regulated by deacetylase SIRT1. Our findings not only provide important information to highlight NMN supplementation as preventive strategy in endotoxin-associated ALI, but also demonstrate potential mechanism insight into NMN pretreatment. The underlying mechanism or pivotal signaling pathways that regulate mitonuclear interaction to alleviate endotoxin-induced ALI will be elucidated in our next study. And, future clinical trials are also required to validate our findings.

AUTHORS' CONTRIBUTIONS

S-HD, JS, and T-YY participated in the design and coordination of the study. J-BY conceived, designed, and organized the study. X-XH, S-MH, Y-YC, Z-LX, and S-SL carried out the animal model and conducted the experiments. S-HD and JS were in charge of writing the manuscript. T-YY, Y-TL, and NL participated in the data interpretation and performed the statistical analysis. All authors read and approved the final manuscript. S-HD, JS, and T-YY contributed equally to this work.

DECLARATION OF CONFLICTING INTERESTS

The author(s) declared no potential conflicts of interest with respect to the research, authorship, and/or publication of this article.

FUNDING

The author(s) disclosed receipt of the following financial support for the research, authorship, and/or publication of this article: This work was supported by the Chinese National Natural Science Foundation (grant nos 82004076 and 81772106) and Youth Science and Technology Project of Tianjin Municipal Health Commission (grant no. QN20027).

ORCID ID

Jian-Bo Yu https://orcid.org/0000-0003-0530-6749

REFERENCES

1. Cecconi M, Evans L, Levy M, Rhodes A. Sepsis and septic shock. *Lancet* 2018;**392**:75–87
2. Martin CM, Priestap F, Fisher H, Fowler RA, Heyland DK, Keenan SP, Longo CJ, Morrison T, Bentley D, Antman N, STAR Registry Investigators. A prospective, observational registry of patients with severe sepsis: the Canadian sepsis treatment and response registry. *Crit Care Med* 2009;**37**:81–8
3. Bellani G, Laffey JG, Pham T, Fan E, Brochard L, Esteban A, Gattinoni L, van Haren F, Larsson A, McAuley DF, Ranieri M, Rubenfeld G, Thompson BT, Wrigge H, Slutsky AS, Pesenti A. Epidemiology, patterns of care, and mortality for patients with acute respiratory distress syndrome in intensive care units in 50 countries. *Jama* 2016;**315**:788–800
4. Gu J, Luo L, Wang Q, Yan S, Lin J, Li D, Cao B, Mei H, Ying B, Bin L, Smith FG, Jin SW. Maresin 1 attenuates mitochondrial dysfunction through the ALX/cAMP/ROS pathway in the cecal ligation and puncture mouse model and sepsis patients. *Lab Invest* 2018;**98**:715–33
5. Shi J, Yu J, Zhang Y, Wu L, Dong S, Wu L, Wu L, Du S, Zhang Y, Ma D. Pi3k/Akt pathway-mediated HO-1 induction regulates mitochondrial quality control and attenuates endotoxin-induced acute lung injury. *Lab Invest* 2019;**99**:1795–809
6. Gomes AP, Price NL, Ling AJ, Moslehi JJ, Montgomery MK, Rajman L, White JP, Teodoro JS, Wrann CD, Hubbard BP, Mercken EM, Palmeira

CM, de Cabo R, Rolo AP, Turner N, Bell EL, Sinclair DA. Declining NAD(+) induces a pseudohypoxic state disrupting nuclear-mitochondrial communication during aging. *Cell* 2013;**155**:1624–38
7. Yun J, Finkel T. Mitohormesis. *Cell Metab* 2014;**19**:757–66
8. Mottis A, Herzig S, Auwerx J. Mitocellular communication: shaping health and disease. *Science* 2019;**366**:827–32
9. Shpilka T, Haynes CM. The mitochondrial UPR: mechanisms, physiological functions and implications in ageing. *Nat Rev Mol Cell Biol* 2018;**19**:109–20
10. Cordeiro AV, Brícola RS, Braga RR, Lenhare L, Silva VRR, Anaruma CP, Katashima CK, Crisol BM, Simabuco FM, Silva ASR, Cintra DE, Moura LP, Pauli JR, Ropelle ER. Aerobic exercise training induces the mitonuclear imbalance and UPRmt in the skeletal muscle of aged mice. *J Gerontol A Biol Sci Med Sci* 2020;**75**:2258–61
11. Mouchiroud L, Houtkooper RH, Moullan N, Katsyuba E, Ryu D, Cantó C, Mottis A, Jo YS, Viswanathan M, Schoonjans K, Guarente L, Auwerx J. The NAD(+)/sirtuin pathway modulates longevity through activation of mitochondrial UPR and FOXO signaling. *Cell* 2013;**154**:430–41
12. Kincaid JW, Berger NA. NAD metabolism in aging and cancer. *Exp Biol Med* 2020;**245**:1594–614
13. Mills KF, Yoshida S, Stein LR, Grozio A, Kubota S, Sasaki Y, Redpath P, Migaud ME, Apte RS, Uchida K, Yoshino J, Imai SI. Long-term administration of nicotinamide mononucleotide mitigates age-associated physiological decline in mice. *Cell Metab* 2016;**24**:795–806
14. Gariani K, Menzies KJ, Ryu D, Wegner CJ, Wang X, Ropelle ER, Moullan N, Zhang H, Perino A, Lemos V, Kim B, Park YK, Piersigilli A, Pham TX, Yang Y, Ku CS, Koo SI, Fomitchova A, Cantó C, Schoonjans K, Sauve AA, Lee JY, Auwerx J. Eliciting the mitochondrial unfolded protein response by nicotinamide adenine dinucleotide repletion reverses fatty liver disease in mice. *Hepatology* 2016;**63**:1190–204
15. Hong G, Zheng D, Zhang L, Ni R, Wang G, Fan GC, Lu Z, Peng T. Administration of nicotinamide riboside prevents oxidative stress and organ injury in sepsis. *Free Radic Biol Med* 2018;**123**:125–37
16. Yu J, Shi J, Wang D, Dong S, Zhang Y, Wang M, Gong L, Fu Q, Liu D. Heme oxygenase-1/carbon monoxide-regulated mitochondrial dynamic equilibrium contributes to the attenuation of endotoxin-induced acute lung injury in rats and in lipopolysaccharide-activated macrophages. *Anesthesiology* 2016;**125**:1190–201
17. Shi J, Yu T, Song K, Du S, He S, Hu X, Li X, Li H, Dong S, Zhang Y, Xie Z, Li C, Yu J. Dexmedetomidine ameliorates endotoxin-induced acute lung injury in vivo and in vitro by preserving mitochondrial dynamic equilibrium through the HIF-1a/HO-1 signaling pathway. *Redox Biol* 2021;**41**:101954
18. Vachharajani VT, Liu T, Brown CM, Wang X, Buechler NL, Wells JD, Yoza BK, McCall CE. Sirt1 inhibition during the hypoinflammatory phenotype of sepsis enhances immunity and improves outcome. *J Leukoc Biol* 2014;**96**:785–96
19. Wu K, Tian R, Huang J, Yang Y, Dai J, Jiang R, Zhang L. Metformin alleviated endotoxemia-induced acute lung injury via restoring AMPK-dependent suppression of mTOR. *Chem Biol Interact* 2018;**291**:1–6
20. Zmijewski JW, Lorne E, Zhao X, Tsuruta Y, Sha Y, Liu G, Siegal GP, Abraham E. Mitochondrial respiratory complex I regulates neutrophil activation and severity of lung injury. *Am J Respir Crit Care Med* 2008;**178**:168–79
21. Nam YK, Jin SC, Kim MH, Choi Y, Lee YB, Yang WM. *Banhahubak*-Tang tablet, a standardized medicine attenuates allergic asthma via inhibition of Janus kinase 1 (JAK1)/ signal transducer and activator of transcription 6 (STAT6) signal pathway. *Molecules* 2020;**25**:2206
22. Mikawa K, Nishina K, Takao Y, Obara H. Efficacy of partial liquid ventilation in improving acute lung injury induced by intratracheal acidified infant formula: determination of optimal dose and positive end-expiratory pressure level. Crit Care Med 2004;**32**:209–16
23. Dahlmans D, Houzelle A, Andreux P, Wang X, Jörgensen JA, Moullan N, Daemen S, Kersten S, Auwerx J, Hoeks J. Microrna-382 silencing induces a mitonuclear protein imbalance and activates the mitochondrial unfolded protein response in muscle cells. *J Cell Physiol* 2019;**234**:6601–10
24. Hong W, Mo F, Zhang Z, Huang M, Wei X. Nicotinamide mononucleotide: a promising molecule for therapy of diverse diseases by targeting NAD+ metabolism. *Front Cell Dev Biol* 2020;**8**:246
25. Jia Y, Kang X, Tan L, Ren Y, Qu L, Tang J, Liu G, Wang S, Xiong Z, Yang L. Nicotinamide mononucleotide attenuates renal interstitial fibrosis after AKI by suppressing tubular DNA damage and senescence. *Front Physiol* 2021;**12**:649547
26. Yoshino J, Baur JA, Imai SI. NAD(+) Intermediates: the biology and therapeutic potential of NMN and NR. *Cell Metab* 2018;**27**:513–28
27. Ying W. NAD+/NADH and NADP+/NADPH in cellular functions and cell death: regulation and biological consequences. *Antioxid Redox Signal* 2008;**10**:179–206
28. Zhang R, Shen Y, Zhou L, Sangwung P, Fujioka H, Zhang L, Liao X. Short-term administration of nicotinamide mononucleotide preserves cardiac mitochondrial homeostasis and prevents heart failure. *J Mol Cell Cardiol* 2017;**112**:64–73
29. Chen L, Li W, Qi D, Wang D. Lycium barbarum polysaccharide protects against LPS-induced ARDS by inhibiting apoptosis, oxidative stress, and inflammation in pulmonary endothelial cells. *Free Radic Res* 2018;**52**:480–90
30. Srivastava A, Shinn AS, Lee PJ, Mannam P. MKK3 mediates inflammatory response through modulation of mitochondrial function. *Free Radic Biol Med* 2015;**83**:139–48
31. Raimundo N. Mitochondrial pathology: stress signals from the energy factory. *Trends Mol Med* 2014;**20**:282–92
32. Fiorese CJ, Schulz AM, Lin YF, Rosin N, Pellegrino MW, Haynes CM. The transcription factor ATF5 mediates a mammalian mitochondrial UPR. *Curr Biol* 2016;**26**:2037–43
33. Cohen HY, Miller C, Bitterman KJ, Wall NR, Hekking B, Kessler B, Howitz KT, Gorospe M, de Cabo R, Sinclair DA. Calorie restriction promotes mammalian cell survival by inducing the SIRT1 deacetylase. *Science* 2004;**305**:390–2
34. Gao R, Ma Z, Hu Y, Chen J, Shetty S, Fu J. Sirt1 restrains lung inflammasome activation in a murine model of sepsis. *Am J Physiol Lung Cell Mol Physiol* 2015;**308**:L847–53
35. Yaku K, Okabe K, Nakagawa T. NAD metabolism: implications in aging and longevity. *Ageing Res Rev* 2018;**47**:1–17
36. Zocchi E, Usai C, Guida L, Franco L, Bruzzone S, Passalacqua M, De Flora A. Ligand-induced internalization of CD38 results in intracellular Ca2+ mobilization: role of Nad+ transport across cell membranes. *FASEB J* 1999;**13**:273–83
37. Wang P, Xu TY, Guan YF, Su DF, Fan GR, Miao CY. Perivascular adipose tissue-derived visfatin is a vascular smooth muscle cell growth factor: role of nicotinamide mononucleotide. *Cardiovasc Res* 2009;**81**:370–80
38. Caton PW, Kieswich J, Yaqoob MM, Holness MJ, Sugden MC. Nicotinamide mononucleotide protects against pro-inflammatory cytokine-mediated impairment of mouse islet function. *Diabetologia* 2011;**54**:3083–92
39. Han X, Tai H, Wang X, Wang Z, Zhou J, Wei X, Ding Y, Gong H, Mo C, Zhang J, Qin J, Ma Y, Huang N, Xiang R, Xiao H. AMPK activation protects cells from oxidative stress-induced senescence via autophagic flux restoration and intracellular NAD(+) elevation. *Aging Cell* 2016;**15**:416–27
40. Li R, Kou X, Geng H, Xie J, Yang Z, Zhang Y, Cai Z, Dong C. Effect of ambient PM(2.5) on lung mitochondrial damage and fusion/fission gene expression in rats. *Chem Res Toxicol* 2015;**28**:408–18
41. De Paepe ME, Gundavarapu S, Tantravahi U, Pepperell JR, Haley SA, Luks FI, Mao Q. Fas-ligand-induced apoptosis of respiratory epithelial cells causes disruption of postcanalicular alveolar development. *Am J Pathol* 2008;**173**:42–56
42. Wang Y, Guo SH, Shang XJ, Yu LS, Zhu JW, Zhao A, Zhou YF, An GH, Zhang Q, Ma B. Triptolide induces sertoli cell apoptosis in mice via ROS/JNK-dependent activation of the mitochondrial pathway and inhibition of Nrf2-mediated antioxidant response. *Acta Pharmacol Sin* 2018;**39**:311–27
43. Kong D, Ding Y, Liu J, Liu R, Zhang J, Zhou Q, Long Z, Peng J, Li L, Bai H, Hai C. Chlorogenic acid prevents paraquat-induced apoptosis via Sirt1-mediated regulation of redox and mitochondrial function. *Free Radic Res* 2019;**53**:680–93
44. Hüttemann M, Helling S, Sanderson TH, Sinkler C, Samavati L, Mahapatra G, Varughese A, Lu G, Liu J, Ramzan R, Vogt S, Grossman

LI, Doan JW, Marcus K, Lee I. Regulation of mitochondrial respiration and apoptosis through cell signaling: cytochrome C oxidase and cytochrome C in ischemia/reperfusion injury and inflammation. *Biochim Biophys Acta* 2012;**1817**:598–609

45. McArthur K, Whitehead LW, Heddleston JM, Li L, Padman BS, Oorschot V, Geoghegan ND, Chappaz S, Davidson S, San Chin H, Lane RM, Dramicanin M, Saunders TL, Sugiana C, Lessene R, Osellame LD, Chew TL, Dewson G, Lazarou M, Ramm G, Lessene G, Ryan MT, Rogers KL, van Delft MF, Kile BT. BAK/BAX macropores facilitate mitochondrial herniation and mtDNA efflux during apoptosis. *Science* 2018;**359**:eaao6047
46. Katsyuba E, Auwerx J. Modulating NAD^+ metabolism, from bench to bedside. *Embo J* 2017;**36**:2670–83
47. Cantó C, Menzies KJ, Auwerx J. NAD(+) metabolism and the control of energy homeostasis: a balancing act between mitochondria and the nucleus. *Cell Metab* 2015;**22**:31–53
48. Ali AT, Boehme L, Carbajosa G, Seitan VC, Small KS, Hodgkinson A. Nuclear genetic regulation of the human mitochondrial transcriptome. *Elife* 2019;**8**:e41927
49. Wang X, Auwerx J. Systems phytohormone responses to mitochondrial proteotoxic stress. *Mol Cell* 2017;**68**:540–15
50. Fu C, Hao S, Xu X, Zhou J, Liu Z, Lu H, Wang L, Jin W, Li S. Activation of Sirt1 ameliorates LPS-induced lung injury in mice via decreasing endothelial tight junction permeability. *Acta Pharmacol Sin* 2019;**40**:630–41
51. Irie J, Inagaki E, Fujita M, Nakaya H, Mitsuishi M, Yamaguchi S, Yamashita K, Shigaki S, Ono T, Yukioka H, Okano H, Nabeshima YI, Imai SI, Yasui M, Tsubota K, Itoh H. Effect of oral administration of nicotinamide mononucleotide on clinical parameters and nicotinamide metabolite levels in healthy Japanese men. *Endocr J* 2020;**67**:153–60

(Received December 8, 2021, Accepted March 28, 2022)